ORIGINAL ARTICLE

WILEY gebiology

Primary productivity of snow algae communities on stratovolcanoes of the Pacific Northwest

T. L. Hamilton[1] | J. Havig[2]

[1]Department of Biological Sciences, University of Cincinnati, Cincinnati, OH, USA

[2]Department of Geology, University of Cincinnati, Cincinnati, OH, USA

Correspondence
T. L. Hamilton, Department of Biological Sciences, University of Cincinnati, Cincinnati, OH, USA. Email: trinity.hamilton@uc.edu

Abstract

The majority of geomicrobiological research conducted on glacial systems to date has focused on glaciers that override primarily carbonate or granitic bedrock types, with little known of the processes that support microbial life in glacial systems overriding volcanic terrains (e.g., basalt or andesite). To better constrain the role of the supraglacial ecosystems in the carbon and nitrogen cycles, to gain insight into microbiome composition and function in alpine glacial systems overriding volcanic terrains, and to constrain potential elemental sequestration or release through weathering processes associated with snow algae communities, we examined the microbial community structure and primary productivity of snow algae communities on stratovolcanoes in the Cascade Range of the Pacific Northwest. Here, we present the first published values for carbon fixation rates of snow algae communities on glaciers in the Pacific Northwest. We observed varying levels of light-dependent carbon fixation on supraglacial and periglacial snowfields at Mt. Hood, Mt. Adams, and North Sister. Recovery of abundant 18S rRNA transcripts affiliated with photoautotrophs and 16S rRNA transcripts affiliated with heterotrophic bacteria is consistent with previous studies indicating the majority of primary productivity on snow and ice can be attributed to photoautotrophs. In contrast to previous observations of glacial ecosystems, our geochemical, isotopic, and microcosm data suggest these assemblages are not limited by phosphorus or fixed nitrogen availability. Furthermore, our data indicate these snow algae communities actively sequester Fe, Mn, and P leached from minerals sourced from the local rocks. Our observations of light-dependent primary productivity on snow are consistent with similar studies in polar ecosystems; however, our data may suggest that DIC may be a limiting nutrient in contrast to phosphorus or fixed nitrogen as has been observed in other glacial ecosystems. Our data underscore the need for similar studies on glacier surfaces and seasonal snowfields to better constrain the role of local bedrock and nutrient delivery on carbon fixation and biogeochemical cycling in these ecosystems.

1 | INTRODUCTION

Today over 15 million square kilometers (5.8 million square miles) of Earth's land surface is covered in ice including glaciers, ice caps, and the ice sheets of Greenland and Antarctica. Glaciers, ice sheets, and snowfields are found on every continent except Australia and are hosted in many different types of bedrock and hydrological regimes. Studies of microbial communities in these ecosystems underscore the role of local bedrock, hydrology, climate, and atmospheric deposition in determining community structure and function (Boetius, Anesio,

Deming, Mikucki, & Rapp, 2015 and references therein). However, the majority of geomicrobiological research has been conducted on glacial systems that override primarily carbonate or granitic bedrock types, with little known of the processes that support microbial life in glacial systems overriding volcanic terrains (e.g., basalt or andesite). Alpine regions of the Pacific Northwest host glaciers and permanent and seasonal snowfields overriding volcanic terrains that range in composition from basalt to dacite, making it an ideal location to elucidate these processes.

Supraglacial snow and snowfields host taxonomically and physiologically diverse microbial populations of eukaryotes, bacteria, and archaea (Boetius et al., 2015 and references therein). On glaciers, snow represents the interface between glacial ice and deposition from aeolian and meteoric precipitation processes, and snow algae communities are the key biological drivers of element uptake and cycling at that interface. Snow algae have been studied extensively in high latitude ice sheets (e.g., Antarctica, Greenland, Iceland, Svalbard) as well as alpine environments (e.g., Alaska, the Himalayas, the Rocky Mountains, and the European Alps) (Boetius et al., 2015 and references therein), while the Cascade Range has received far less attention. A recent study examined snow algae biogeography in the Glacier Peak Wilderness Area in northern Washington (Brown, Ungerer, & Jumpponen, 2016), and others are currently underway in the North Cascades National Park as a part of a BioBlitz program (R. Kodner, unpublished data); but the geomicrobiology and in situ activity of microbial populations found on glaciers in the Cascade Range of the Pacific Northwest has not been characterized.

Glaciers on stratovolcanoes such as those in the Cascade Range of the Pacific Northwest may provide unique ecosystems compared with glaciers that override granitic or carbonate-rich bedrock although these studies are limited. Recent eruptions and rapid glacial retreat result in snow and ice ecosystems in the Cascade Range that receive wind-blown volcanic ash and rock flour. On Icelandic glaciers, vicinity to active glaciers results in delivery of fresh ash which is an important source of essential nutrients (Lutz, Anesio, Edwards, & Benning, 2015). In Iceland, both snow algae pigmentation and volcanic ash are reducing surface albedo which may accelerate melt rate. In the Cascade Range, glaciers are particularly susceptible to rising temperatures due to their size and location (mid-latitude) and are experiencing rapid retreat. Based on 20th century glacier loss rates of ~0.29 km^2/yr for Mt. Rainier, the Sisters in Oregon may be glacier-free in only ~20 years, and Mt. Hood in OR and Mt. Adams in WA in ~80 years (data from the Portland State University Glaciers of the American West Database). However, the role of snow algae and delivery of debris and ash on surface albedo and melt rates to these surfaces remains poorly understood.

High microbial activity has been observed on glacial surfaces (Anesio, Hodson, Fritz, Penner, & Sattler, 2008). Blooms of photosynthetic algae and cyanobacteria are often visible on snow or ice surfaces, turning the snow or ice surfaces red, pink, green, yellow, and orange. These photoautotrophs serve as predominant primary producers in many glacial and snowfield ecosystems (Hodson et al., 2008) where only a few specialized phototrophs thrive in the high-irradiation environment with average temperatures near the freezing point (Morgan-Kiss, Priscu, Pocock, Gudynaite-Savitch, & Huner, 2006; Remias, Karsten, Lütz, & Leya, 2010). In addition to supporting local microbial communities and multicellular life and feeding into the subglacial environment and glacial meltwater, satellite imaging and primary productivity measured in situ suggest photoautotrophic populations hosted on snow in supraglacial ecosystems are a significant component of the modern global carbon cycle (Anesio et al., 2008; Cook et al., 2012; Hisakawa et al., 2015; Takeuchi, Dial, Kohshima, Segawa, & Uetake, 2006). There is also evidence that microbial assemblages on glacial surfaces actively cycle nitrogen (Boyd et al., 2011; Hamilton, Peters, Skidmore, & Boyd, 2013; Hodson et al., 2008). Primary productivity in supraglacial ecosystems (on the ice and snow surface) appears to be nutrient- and temperature-limited (Hodson et al., 2008). Phosphorous limitation has been reported in glacial environments (Edwards et al., 2013; Stibal, Anesio, Blues, & Tranter, 2009) and there is evidence that biologically available (fixed) nitrogen is also limiting on glaciers and ice sheets (Boyd et al., 2011; Stibal, Šabacká, & Kaštovská, 2006; Telling et al., 2011).

Despite the role of supraglacial and snowfield microbial communities in local and global biogeochemical cycling and foodwebs, relatively few studies have measured photoautotrophic primary productivity in snow algae communities on glaciers and snowfields (Hodson et al., 2010; Stibal, Šabacká, & Žársky, 2012a; Stibal et al., 2012b; Thomas & Duval, 1995). Furthermore, none have reported carbon fixation for snowfields on or near glaciers in the Cascade Range of the Pacific Northwest. Nutrient dynamics including local geology and anthropogenically derived nitrogen deposition on snow and ice surfaces remains largely uncharacterized (Hodson et al., 2008; Telling et al., 2011) as does the delivery of nutrients, cells, and debris from the snow and glacial ice to the surrounding landscape and subglacial sediments. Because extant glaciers are built from years of accumulated snow, and biological activity within glacial ice is likely negligible, extant supraglacial communities serve as a proxy for the geochemical attributes of ancient snow algae communities entombed in the glacial ice.

Here, we report the recovery and composition of 16S and 18S rRNA transcripts from supra- and periglacial snow on three separate stratovolcanoes of the Pacific Northwest as well primary productivity and element sequestration by these assemblages. This study is one of only a handful to report the recovery and analyses of RNA from glacial microbial communities (Boyd, Hamilton, Havig, Skidmore, & Shock, 2014; Hamilton et al., 2013). Our data indicate that the majority of primary productivity on supraglacial and periglacial snow is light dependent and can be largely attributed to the activity of eukaryotic algae. This observation is supported by bulk ^{13}C isotopes of the biomass collected from these sites which reflects a signature that typically corresponds to carbon fixation using the pentose phosphate cycle (i.e., the Calvin cycle). Despite previous observations that supraglacial communities are limited in fixed nitrogen and/or phosphorous, addition of nitrate, ammonium, or phosphate to our microcosms did not uniformly stimulate carbon fixation rates in our microcosms. Furthermore, our data suggest snow algae communities are sequestering Fe, P, and Mn sourced from local lava and volcanic ash. Collectively, our data support

a role of supraglacial and periglacial snow algae photosynthesis contributing fixed carbon to the local ecosystem and highlight a role for local bedrock in supplying key nutrients to support photoautotrophic carbon fixation on supraglacial and periglacial snow.

2 | MATERIALS AND METHODS

2.1 | Field site descriptions

Samples were collected from several sites within the Cascade Volcano Arc: Mount Adams in Washington, and Mount Hood and North Sister in Oregon in June of 2015 (Figure 1). On Mount Hood, samples were collected from Palmer Glacier (121°42′W, 45°21′N) on June 20 and Eliot Glacier (121°42′W, 45°21′N) on June 22. On Mount Adams, samples were collected from a snowfield near Mazama Glacier (121°27′W, 46°9′N) and from Gotchen Glacier (121°27′W, 46°9′N) on June 21. On North Sister, samples were collected from Collier Glacier (121°47′W, 44°10′N) on June 25. The weather on all sampling days was sunny and clear with limited high-altitude clouds.

Mount Adams is a Quaternary composite stratovolcano composed of older basalt flows with a central peak that is basaltic andesite and andesite, with a very minor dacite component (Hildreth & Lanphere,

1994). Of the three sites, Mt. Adams represents a middle composition between the more silicic Mt. Hood and the more mafic North Sister (both described below). Mount Adams is the most voluminous stratovolcano in the Cascades (second only to Mt. Shasta in CA) and is the largest active volcano in Washington State. It has over 200 perennial snow and ice features and twelve glaciers. Total glacier area on Mount Adams has decreased 49% since 1904 (Sitts, Fountain, & Hoffman, 2010). Gotchen and Mazama Glaciers are located on the southeastern side of Mount Adams. Gotchen Glacier is the smallest ice sheet on Mount Adams and has decreased in size by 78% since 1904 (Sitts et al., 2010). Manama Glacier has decreased in size by 46% since 1904 (Sitts et al., 2010).

Mount Hood is an active Quaternary composite stratovolcano in the Cascade Mountains of northern Oregon composed primarily of olivine-, pyroxene-, and hornblende-dacite lavas and pyroclastic flows with smaller eruptions of hornblende andesite and olivine andesite and olivine basalt (Wise, 1969). Of the three sampling areas, Mt. Hood is the most silicic in composition. Palmer Glacier is on the south slope of Mount Hood. The glacier extends from 2,800 to 1,900 m above sea level and is within the Timberline ski area. Palmer Glacier lost 70% of its debris-free ice area from 1987 to 2005, but the lower portion of the glacier is subject to artificial maintenance and anthropogenic input
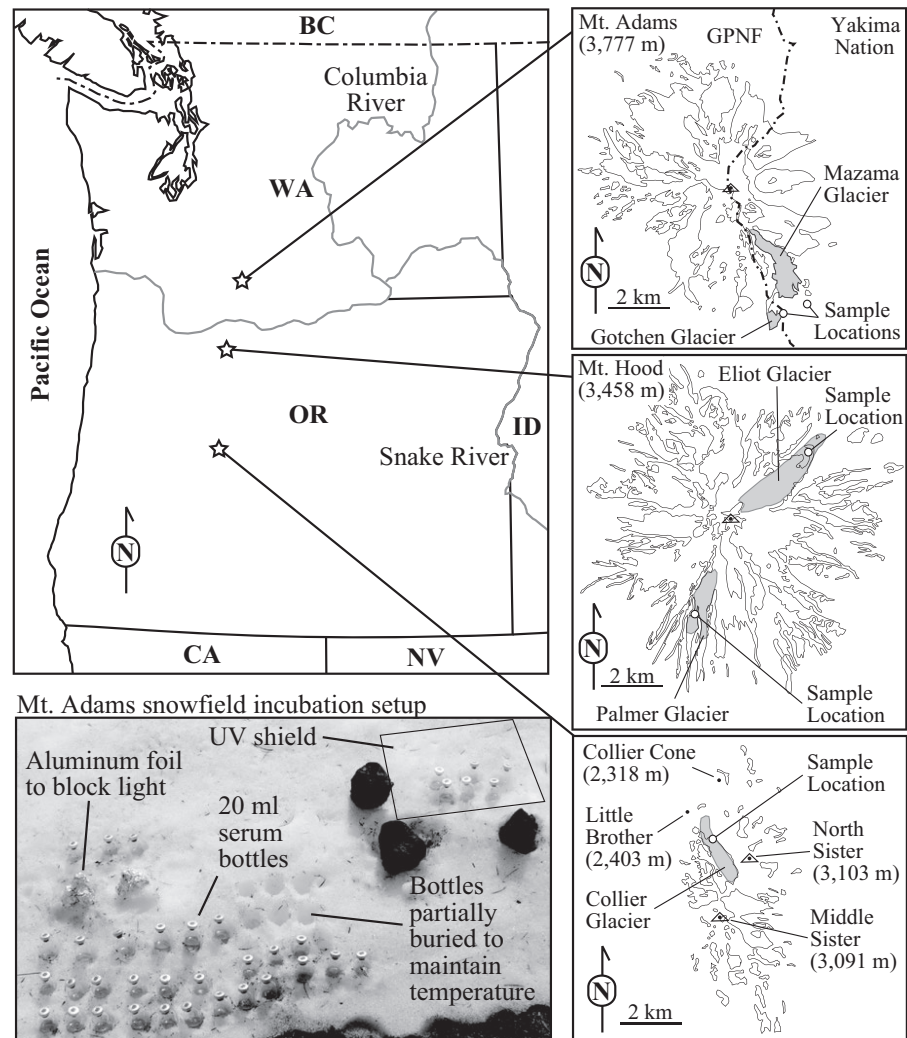

FIGURE 1 Map of sampling site locations and the microcosm setup

as part of the Timberline Ski Resort. Eliot Glacier is a 1.6 km^2 glacier on the northeastern side of Mount Hood. The glacier is littered with rock debris as a result of frequent rock avalanches from north face of Mount Hood which is geothermally altered. Since 1901, Eliot Glacier has retreated 680 m and lost 19% of its area (Jackson & Fountain, 2007); however, it has retreated at a slower rate than the other glaciers on Mount Hood.

North Sister is the oldest of the Three Sisters volcano complex in central Oregon and is considered extinct. North Sister is a composite stratovolcano primarily composed of basaltic andesite and is more mafic than the two adjacent volcanoes (Middle and South Sisters), as well as Mt. Adams and Mt. Hood (Schmidt & Grunder, 2011). The compositional homogeneity of the North Sister stands out in contrast to those of other long-lived stratovolcanoes of the High Cascades, which tend to have compositions that range from basaltic through to rhyodacitic throughout their eruptive history (Mercer & Johnston, 2008). Collier Glacier is on the west side of North Sister and reaches across Middle and North Sister. It has retreated more than 50% since the 1930s.

2.2 | Sample collection

Sediments or snow/ice for RNA extraction was collected in triplicate using a flame-sterilized spatula and placed in sterile 1.5-ml microcentrifuge tubes. Supraglacial and periglacial sites with orange, green, pink, or red hues indicative of snow algae communities were targeted for collection. Samples were immediately flash-frozen on dry ice. For bulk geochemical analyses (described in detail below), approximately 1 L volume of the surface layer of the snow was collected from the same site as was used for incubations (detailed below) using a sterile spatula and placed in a clean 1-L polypropylene bottle (soaked in 10% trace-element-grade HNO$_3$ for 3 days, triple-rinsed with 18.2 MΩ/cm deionized water), and the snow was melted in the closed bottle with minimal atmospheric exposure to facilitate filtration but minimize exchange of CO$_2$ with the atmosphere.

2.3 | Snow and snow algae geochemistry

Temperature, conductivity, and pH were measured in the thawed snow onsite using a WTW 330i meter and probe (Xylem Analytics, Weilheim, Germany), and conductivity and temperature were measured with a YSI 30 conductivity meter and probe (YSI, inc., Yellowsprings, OH, USA). All water samples were filtered through 25-mm-diameter 0.2-µm polyethersulfone syringe filters (VWR International, Radnor, PA, USA). Samples for ion chromatography analysis of anions were filtered into 15-ml centrifuge tubes that had been pre-soaked in 18.2 MΩ/cm DI water, and stored at 4°C until analysis. Major anions (fluoride, chloride, sulfate, and nitrate) were determined using a Dionex ICS 1600 ion chromatograph by the STAR Lab (the Ohio State University). Samples for cation (sodium, potassium, calcium, and magnesium) and total dissolved trace element (phosphorous, manganese, and iron) analysis (10 ml) were filtered into acid-washed (three-day soak in 10% TraceMetal Grade HNO$_3$ (Fisher Scientific, Hampton, NH) followed by

triple rinsing with 18.2 MΩ/cm DI water) 15-ml centrifuge tubes and acidified with 400 µl of concentrated OmniTrace Ultra™ concentrated nitric acid (EMD Millipore, Billerica, MA, USA), and stored at 4°C until analysis. Approximately 30 ml of sample was flushed through the filter before the trace element sample was collected. Analysis was conducted via Teledyne Leeman Labs Prodigy Dual view inductively coupled plasma optical emission spectrometer (ICP-OES) (Teledyne Leeman Labs, Hudson, New Hampshire, USA) by the STAR Lab at the Ohio State University. Field blanks (18.2 MΩ/cm deionized water transported to the field in acid-washed one-liter Nalgene bottles) were taken daily using the same equipment and techniques described above as checks for contamination.

Samples for dissolved inorganic carbon (DIC) concentration analysis were filtered into Labco Exetainers® (Labco Limited, Lampeter, UK) until there was no head space, and then kept refrigerated until analysis. Analyses were conducted by the Stable Isotope Facility at University of California, Davis, using a GasBench II system interfaced to a Delta V Plus isotope ratio mass spectrometer (IR-MS) (Thermo Scientific, Bremen, Germany) with raw delta values converted to final using laboratory standards (lithium carbonate, $\delta^{13}C$ = −46.6‰ and a deep sea water, $\delta^{13}C$ = +0.8‰) calibrated against standards NBS-19 and L-SVEC.

Samples for dissolved organic carbon (DOC) concentration analysis were filtered into 50-ml centrifuge tubes (final volume 25–30 ml), flash-frozen on dry ice, and stored at −20°C until analysis. Analyses were conducted by the Stable Isotope Facility at University of California, Davis, using O.I. Analytical Model 1030 TOC Analyzer (O.I. Analytical, College Station, TX) interfaced to a PDZ Europa 20-20 isotope ratio mass spectrometer (Sercon Ltd., Cheshire, UK) utilizing a GD-100 Gas Trap Interface (Graden Instruments) for concentration and isotope ratio determination with raw delta values converted to final using laboratory standards (KHP and cane sucrose) calibrated against USGS-40, USGS-41, and IAEA-600.

Subsets of incubation bulk snow algae samples were dried (60°C for 3 days) and ground/homogenized with a cleaned mortar and pestle (ground with ethanol silica slurry, triple-rinsed with 18.2 MΩ/cm deionized water, dried). Samples were sent to the STAR Lab at the Ohio State University where they were digested in a concentrated HNO$_3$–HCl solution (following EPA method 3051) using a CEM MARS Express microwave digestion system (CEM Corporation, Matthews, NC, USA). Following digestion, samples were analyzed for elemental composition (Na, Mg, Al, P, S, K, Ca, Mn, Fe) using the ICP-OES system described above. Bulk snow algae samples include all sediments and allochthonous material not large enough to be seen by the naked eye and removed. Bulk samples were analyzed for C and N concentration and isotopic signature via EA-IR-MS as described below.

2.4 | CO$_2$ photoassimilation

Inorganic carbon uptake was assessed in situ using a microcosm-based approach through the addition of NaH^{13}CO$_3$. In areas of snow and ice where phototrophic populations were visibly apparent (green- or

red-colored snow), samples were collected from the surface layer using a pre-sterilized spatula, placed into a clean container, and allowed to melt to a slush slurry. An equal volume (~ 15 ml) of snow slush slurry was then transferred into pre-combusted (12 h, 450°C) serum vials and capped with gas-tight black butyl rubber septa. Assays were initiated by addition of $NaH^{13}CO_3$ (100 µM final concentration) (Cambridge Isotope Laboratories, Inc., Andover, MA, USA). All assays were performed in triplicate.

At each site, we assessed the potential for photoautotrophic (light) and chemoautotrophic (dark) $NaH^{13}CO_3$ uptake (Figure 1). To assess CO_2 assimilation in the dark, vials ($n = 3$) were amended with $NaH^{13}CO_3$ and completely wrapped in aluminum foil. To assess nutrient limitation, a subset of vials were amended with $NaNO_3$, NH_4Cl, or KH_2PO_4 (final concentration 500 µM). To assess the effects of ultraviolet radiation, vials ($n = 3$) were placed under a sheet of acrylic which blocks 99% all UVA and UVB (Figure 1). Natural abundance controls were amended with unlabeled $NaHCO_3$ (Sigma-Aldrich, St Louis, MO, USA). All assays were performed in triplicate and reported values of DIC uptake (carbon fixation rates) reflect the difference in uptake between the labeled and unlabeled assays. All calculations for carbon uptake analyses were based on the difference between treatments and unamended biomass collected at the time of sampling. Unamended biomass values are reported in Table 1. Photosynthetically active radiation (PAR) was measured at the surface at several time points during each incubation using a BiTec Sensor Luxometer (Gigahertz-Optik, Newburyport, MA, USA).

2.5 | C and N concentration and stable isotope signals

Following incubation, samples were filtered onto pre-combusted (12 h, 450°C) GF/F filters (0.3-µm pore size) (Sterlitech Corporation, Kent, WA, USA), flushed with HCl (1 M) to remove any carbonate minerals, washed with de-ionized H_2O, and dried (8 h, 60°C). Dried and ground bulk samples or filtered and dried incubation samples for the determination of C and N concentration and stable isotope signal were weighed and placed into tin boats, sealed, and analyzed via a Costech Instruments Elemental Analyzer (EA) periphery connected to a Thermo Scientific Delta V Advantage Isotope Ratio Mass Spectrometer (IR-MS) at the Stable Isotope Geochemistry Lab in the Department of Geology at the University of Cincinnati. Linearity corrections were made using NIST Standard 2710, and $\delta^{13}C$ values were calibrated using reference standards USGS-40 and USGS-41 and checked with a laboratory standard (glycine). Total uptake of DIC was calculated using DIC numbers determined for the source water (snow) (described above). All stable isotope results are given in delta formation expressed as per mil (‰). Carbon stable isotopes are calculated as:

$$\delta^{13}C = [((R_a)_{sample}/(R_a)_{standard}) - 1] \times 10^3, \qquad 1$$

where R_a is the $^{13}C/^{12}C$ ratio of the sample or standard, and are reported versus the Vienna Pee Dee Belemnite (VPDB) standard,

while for nitrogen $\delta^{15}N$ values, R_a is the $^{15}N/^{14}N$ ratio of the sample or standard, and are reported versus atmospheric air.

We have chosen to report the results of our carbon uptake experiments in units relating to the mass of organic carbon in the material used for the incubations, reported here as micrograms of carbon incorporated (µg C) per gram of carbon in the incubation material (g $C_{biomass}$) per hour. These units allow direct comparison of carbon uptake rates based on easily quantifiable values (amount of carbon in a sample). We have avoided presenting the results in per unit surface area or per unit volume due to the heterogeneous nature of supraglacial systems in terms of amount of biomass per unit area or volume. We chose to use per hour (with specific time of day and irradiance during the incubation) instead of per day rates to avoid inconsistency in length of the day (and thus photosynthetically active radiation) in the Northern Hemisphere which can change dramatically depending on time of year. For comparisons between mean ^{13}C uptake rates at each site, a one-way ANOVA followed by post hoc pairwise comparisons between treatments was conducted using a Turkey honest significant difference (HSD) within the R software package (R version 3.2.4, R Foundation for Statistical Computing, Vienna, Austria). Mean rates with p-values $<.05$ were considered significantly different.

2.6 | RNA extraction and generation of complementary DNA (cDNA)

RNA extraction and purification were carried with a FastRNA Spin kit for Soil (MP Biomedicals) as described previously (Hamilton et al., 2013). RNA was extracted in triplicate from three independent ~500 mg subsamples of biomass/sediments. Equal volumes of each triplicate extraction were pooled for further analyses. In addition to the biomass/sediment samples, RNA extraction and purification were carried on negative controls consisting of 18.2 MΩ/cm deionized water placed in sterile 1.5-ml microcentrifuge tubes in the field or no sample (extraction blank). No RNA or DNA was detected in the negative controls (see Qubit and PCR methods below) and sequencing of samples failed to generate amplicons. After initial purification, RNA was subjected to DNase I digestion (Roche, Indianapolis, IN, USA) for 1 h at room temperature (~22°C). Following digestion, RNA was further purified using a High Pure RNA Isolation Kit (Roche) and was stored at −80°C in a solution of 100% ethanol and 0.3 M sodium acetate until further processed. The concentration of RNA was determined using a Qubit RNA Assay kit (Molecular Probes, Eugene, OR, USA) and a Qubit 3.0 Fluorometer (Life Technologies, Carlsbad, CA, USA). Following DNase I digestion, RNA extracts were screened for the presence of contaminating genomic DNA by performing a PCR using ~1 ng of RNA as template and primers targeting 16S rRNA gene sequences (515f) (Caporaso et al., 2012) and the recently modified 806rB (Apprill, McNally, Parsons, & Weber, 2015) and primers targeting 18S rRNA gene sequences (euk7F/507R) (Weekers, Gast, Fuerst, & Byers, 1994).

cDNA was synthesized from 20 ng of purified RNA using the Superscript IV Reverse Transcriptase (Life Technologies, Carlsbad, CA, USA) according to the manufacturer's instructions. Following

TABLE 1 Aqueous geochemistry of snow samples and bulk geochemistry of snow algae samples (including associated sediments)[a,b]

	Snow field Mt.Adams, WA	Gotchen Glacier Mt.Adams, WA	Palmer Glacier Mt. Hood, OR	Eliot Glacier Mt. Hood, OR	Collier Glacier North Sister, OR
Incubaion	Y	N	N	Y	Y
GPS					
10 T	0619597	0618966	0601163	0604133	0596793
UTM	5113175	5113567	5022830	5026631	4891529
Error	2.8 m	2.8 m		2.8 m	2.8 m
Elevation	2078 m	2211 m	2327 m	2105 m	2287 m
Time	13:15	17:30	17:45	14:18	08:00
Date	06/21/15	06/21/15	06/20/15	06/22/15	06/25/15
Aqucous geochemistry					
pH	5.60	5.59	4.72	5.50	6.48
Temperature	0.0–2.0°C	0.0°C	0.0°C	0.5–6.0°C	1.0–5.0°C
Conductivity	3.75 µS/cm	2.75 µS/cm	12.25 µS/cm	2.57 uS/cm	10.99 uS/cm
DIC	56.9 µM	84.0 µM	44.0 µM	13.9 µM	52.5 µM
$\delta^{13}C$	bdl	−17.70[b]	bdl	bdl	bdl
DOC	297.6 µM	276.5 µM	101.0 µM	107.5 µM	289.0 µM
$\delta^{13}C$	−25.83‰	−23.18‰	−27.22‰	−27.35‰	−26.44‰
Fluoride	bdl	bdl	2.3 µM	bdl	2.1 µM
Chloride	9.4 µM	15.1 µM	4.4 µM	9.5 µM	4.3 µM
Sulfate	bdl	4.1 µM	5.0 µM	5.2 µM	4.5 µM
Nitrate	bdl	bdl	5.7 µM	bdl	0.4 µM
Phosphorous	1.0 µM	bdl	bdl	bdl	1.4 µM
Sodium	6.6 µM	18.4 µM	6.2 µM	7.8 µM	24.9 µM
Potassium	7.7 µM	10.1 µM	bdl	7.4 µM	bdl
Calcium	bdl	0.8 µM	4.0 µM	10.0 µM	9.2 µM
Magnesium	0.6 µM	0.8 µM	0.5 µM	0.3 µM	6.2 µM
Manganese	32.8 nM	20.0 nM	21.8 nM	18.2 nM	bdl
Iron	bdl	bdl	−734.2 nM	46.6 nM	bdl
Bulk snow algae samples					
Total C	29.66%	6.14%	3.29%	0.98%	0.97%
$\delta^{13}C$	−26.20‰	−24.09‰	−25.87‰	−26.85‰	−26.54‰
Total N	1.47%	0.41%	0.16%	0.09%	0.06%
$\delta^{15}N$	−4.09‰	−3.76‰	−6.20‰	−4.54‰	−4.11‰
Phosphorous	42.6 mM	13.4 mM	12.4 mM	12.7 mM	6.4 mM
Iron	201.5 mM	175.5 mM	173.6 mM	224.4 mM	399.4 mM
Manganese	2.4 mM	1.9 mM	1.4 mM	1.9 mM	5.2 mM
Sulfur	34.4 mM	11.0 mM	8.5 mM	8.4 mM	13.4 mM
Sodium	27.1 mM	28.1 mM	51.3 mM	38.5 mM	95.1 mM
Magnesium	96.5 mM	122.8 mM	25.9 mM	38.8 mM	520.6 mM
Aluminum	303.5 mM	139.7 mM	176.7 mM	145.6 mM	594.0 mM
Potassium	48.7 mM	13.9 mM	13.1 mM	11.2 mM	18.9 mM
Calcium	47.8 mM	53.6 mM	66.6 mM	56.5 mM	265.5 mM

DIC, dissolved inorganic carbon; bdl, below detection limits. Carbon isotope values given vs. VPDB, nitrogen values given vs. air.
[a]Method detection limits: 13C—100 µM; fluoride—1.4 µM; sulfate—1.4 µM; phosphorus—0.52 µM; potassium—4.6 µM; calcium—0.77 µM; magnesium—0.12 µM; manganese—18.2 nM; iron (total Fe)—17.9 nM.
[b]Italic value represents qualitative estimates only.

synthesis of cDNA, samples were purified by ethanol precipitation and resuspended in nuclease-free water for use in amplicon sequencing.

2.7 | Sequence analysis

Amplicons were sequenced using MiSeq Illumina 2 × 300 bp chemistry using the primers 515Ff and 806rB targeting V4 hypervariable region of bacterial and archaeal 16S SSU rRNA gene sequences and primers euk7F and 507R targeting eukaryotic 18S rRNA gene sequences by the Research and Testing Laboratory (Lubbock, TX, USA). Each sample was sequenced once. Post-sequence processing was performed using the Mothur (ver. 1.36.1) sequence analysis platform (Schloss et al., 2009) following the MiSeq SOP (Kozich, Westcott, Baxter, Highlander, & Schloss, 2013). For the 18S rRNA data set, we analyzed the forward read only as well as the assembled contigs. For the 16S rRNA data set, read pairs were assembled. Contigs with ambiguous bases were removed. Contigs were trimmed to include only the overlapping regions and unique sequences were aligned against the SILVA v119 database. Chimeras were identified and removed using UCHIME (Edgar, Haas, Clemente, Quince, & Knight, 2011). Operational taxonomic units (OTUs) were assigned at a sequence similarity of 0.97 using the average neighbor method. OTUs were classified within Mothur against the SILVA database (v119) with Mothur using the naive Bayesian algorithm and manually verified with BLASTN (Altschul et al., 1997). Rarefaction was calculated within Mothur and based on rarefaction analysis, >92% of the predicted 16S and 18S rRNA gene diversity was sampled at this depth of sequencing (data not shown). Results were visualized with the Phyloseq R package (ver. 1.16.2; McMurdie & Holmes, 2013) (R version 3.2.4). The OTUs recovered, OTU abundance, and taxonomic classification of 18S rRNA analyses were similar (forward reads only or merged reads) and here we report data from the assembled contigs.

2.8 | Nucleotide sequence accession numbers

Sequence data including raw reads, quality scores, and mapping data have been deposited in the NCBI Sequence Read Archive (SRA) database with the accession number SRP076975. Library designations and samples sites are provided in Table S1.

3 | RESULTS

3.1 | Snow geochemistry

Supraglacial and periglacial snow samples containing snow algae were collected from several sites within the Cascade Volcano Arc: basaltic to andesitic Mount Adams in Washington, and dacitic Mount Hood and basaltic-andesitic North Sister in Oregon during June of 2015 (Figure 1). On Mount Adams, samples were collected from snowfields downslope from Mazama and Gotchen Glaciers. On Mount Hood, samples were collected from the surface of Palmer Glacier and Eliot Glacier. On North Sister, samples were collected from the surface of Collier Glacier. For all supraglacial and periglacial samples, pH ranged

from 4.7 to 6.5 (Table 1). Collier and Palmer Glacier samples had elevated conductivity (10.66 and 12.25 μS/cm) compared with Eliot Glacier and Mt. Adams snow (2.57–3.75 μS/cm). Levels of nitrate were similar in all samples, with concentrations at or below 5.7 μM. Ammonia was below detection limits in all samples (data not shown). Chloride concentrations ranged from 4.3 to 15 μM, while sulfate concentrations ranged from 5.2 μM to below detection limits. Total dissolved phosphorous was only above detection limits in the Mt. Adams and Collier Glacier samples (1.0 and 1.4 μM, respectively). Magnesium concentration ranged from 0.3 to 6.2 μM. Calcium was also detected in μM concentrations from all samples except the Mount Adams snow. Total dissolved iron was only detected in snow from Eliot Glacier (46.6 nM) and Palmer Glacier (734.2 nM). Total dissolved manganese was present in nM concentrations in all sites except in Collier Glacier snow where it was not detected. The concentration of dissolved inorganic carbon (DIC) was lowest in the Gotchen Glacier snow sample (0.1 μM) and ranged from 13.9 to 56.9 μM in the other samples. Dissolved organic carbon concentrations ranged from 101 μM in the Palmer Glacier sample to 289 μM in the Collier Glacier sample.

3.2 | Geochemical analysis of bulk snow algae community biomass

Bulk snow algae biomass samples ranged from a high of 29.66% C and 1.47% N (Gotchen Glacier snow, Mt. Adams) to lows of 0.98% C, 0.09% N (Eliot Glacier snow, Mt. Hood) and 0.97% C, 0.06% N (Collier Glacier snow, North Sister), with the other sites falling between (Table 1). All percentages are relative to total dry mass of bulk snow algae samples, with low total carbon values indicative of a large volcanic sediment component. Snow algae samples displayed δ^{13}C values ranging from −24.1‰ to −26.9‰ (vs. VPDB), consistent with those reported for carbon via the pentose phosphate cycle (i.e., the Calvin cycle) (Havig, Raymond, Meyer-Dombard, Zolotova, & Shock, 2011) which is employed by eukaryotic photoautotrophic algae and cyanobacteria. Snow algae δ^{15}N values ranged from −3.8‰ to −6.2‰ (vs. air) (Table 1), similar to those observed in δ^{15}N values from an atmospheric precipitation fixed nitrogen source (Moore, 1977). Phosphorous concentration in the bulk snow algae samples ranged from a high value of 42.3 mM (Mt. Adams snowfield sample) to a low of 6.4 mM (Collier Glacier site) (Table 1). Total iron in the samples was circum 200 mM, with only the Collier Glacier site deviating (399.4 mM). Manganese concentrations fell between 1.4 and 5.2 mM. Total sulfur concentrations fell between 34.4 and 8.4 mM. For the other major rock-forming elements measured (Na, Mg, Al, K, and Ca), concentrations were generally lowest at the Mt. Hood sites, highest at the North Sister site, with Mt. Adams falling between the two, reflecting the general trend in rock type (Mt. Hood being the most felsic, Mt. Adams being intermediate, and North Sister being the most mafic).

3.3 | Snow and sediment community composition

Sequencing of SSU cDNA from supraglacial ecosystems and surrounding sediments revealed the presence of active eukarya, bacteria,

and archaea. We recovered a total of 2698 distinct eukaryal OTUs (defined at 3.0% sequence dissimilarities). The majority of eukaryal OTUs recovered were affiliated with Chlorophyceae (green algae). Chlorophyceae-affiliated sequences were recovered from both surface ice-associated and snowfield samples as well as surrounding sediments (Figure 2; Table S6). The most abundant Chlorophyceae OTUs were affiliated with the Genus *Chlamydomonas* and *Chloromonas*. BLASTN analyses of these OTUs returned sequences recovered from alpine snow, seasonal snow pack, and supraglacial snow (Table S6). In addition, we observed some 18S rRNA transcripts affiliated with the Chrysophyceae, a class of golden algae; however, these sequences were much less abundant. Sequences affiliated with Agaricomycetes and Agaricostilbomycetes, fungi within the Basidiomycota, were abundant in sediments adjacent to Gotchen Glacier and Collier Glacier, respectively. Basidiomycetous yeasts are often cold tolerant and successfully colonize extremely cold habitats including glaciers and high-altitude regions (Branda et al., 2010).

We recovered a total of 2445 distinct bacterial OTUs (defined at 3.0% sequence dissimilarity). The most abundant OTUs we recovered were from 16S rRNA transcripts affiliated with Bacteroidetes, within the Sphingobacteria and Betaproteobacteria (Figure 2; Table S7), which are common constituents of snow algae communities. For instance, Betaproteobacteria were abundant in samples from Iceland, whereas Sphingobacteria were abundant in samples from Northern Sweden (Lutz et al., 2016). The most abundant Bacteroidetes OTUs were affiliated with the genus *Solitalea* and *Ferruginibacter* (Table S7). The majority of the Betaproteobacteria 16S rRNA SSU cDNA sequences recovered from the snow and ice samples were affiliated with the order Burkholderiales and the genus *Polaromonas*. *Polaromonas* spp. are commonly observed in samples from glacial surfaces, snow, and sediments (Darcy, Lynch, King, Robeson, & Schmidt, 2011; Hell et al., 2013; Michaud et al., 2012). Based on BLASTN analyses, the most abundant Bacteroidetes OTUs were most closely related to sequences recovered from glaciers and freshwater biofilms, whereas the sequences affiliated with the genus *Polaromonas* were most closely related to sequences recovered from a drinking water treatment plant and Lake Taihu (Table S7). Transcripts affiliated with Alphaproteobacteria and Actinobacteria were also recovered from all samples. 16S rRNA transcripts affiliated with Cytophagia were abundant in Collier Glacier sediments. The Cytophagia sequences were most closely related to *Hymenobacter* spp., which have been observed on other glaciers (Zhang, Yang, Wang, & Hou, 2009; Klassen & Foght, 2011) and in "red snow" in Antarctica (Fujii et al., 2010). *Hymenobacter*-like strains isolated from basal ice of Victoria Upper Glacier, Antarctica, were psychrotolerant and heterotrophic aerobes (Klassen & Foght, 2011).

Fewer OTUs affiliated with archaea were recovered compared with bacteria and eukarya (Figure 2; Table S8). We recovered 89 archaeal OTUs (defined at 3.0% sequence dissimilarities). This observation suggests bacteria and eukarya are the dominant active fraction of surface microbial assemblages in glacial snow and ice in these systems. Sequences affiliated with the Soil Crenarchaeotic Group (SCG) were recovered in Mt. Adams snow and sediments as well as the surface of Palmer Glacier and sediments from Gotchen Glacier and Collier Glacier.
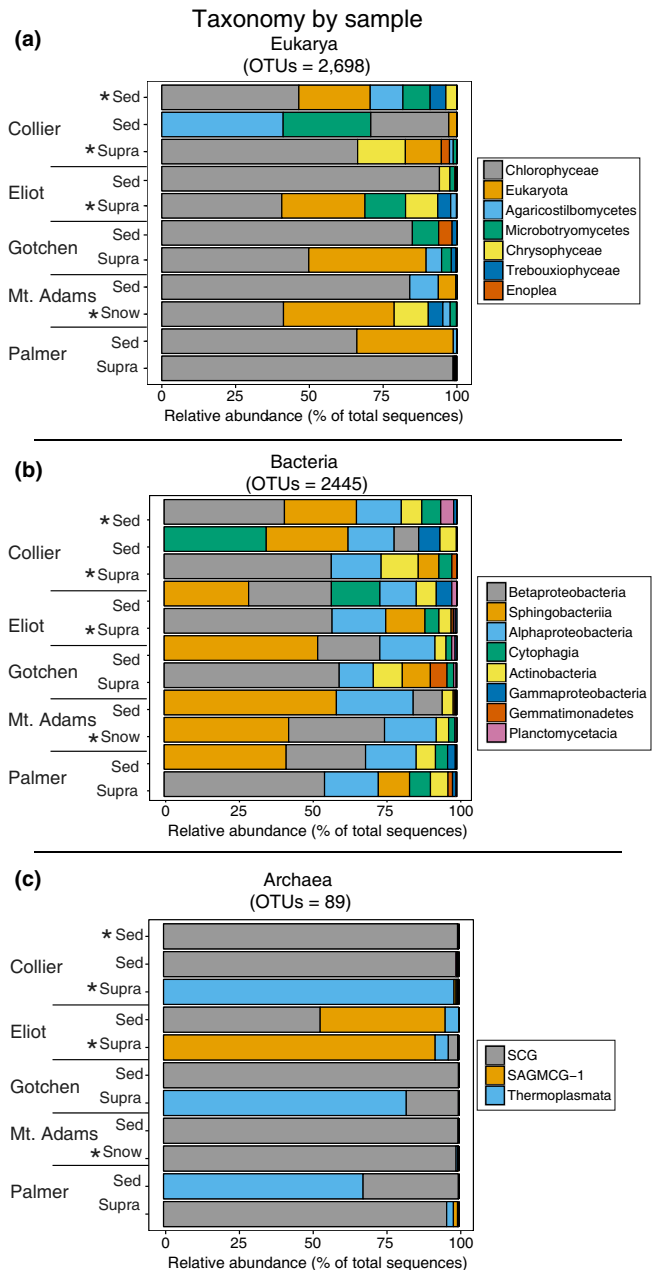

FIGURE 2 Composition of small subunit rRNA transcripts recovered from sediment (Sed) and supraglacial snow or snowfield samples (Snow). OTUs for each library were binned at the class level for archaea and bacteria and at the order level for eukarya. For eukarya and bacteria, only OTUs which were present in 50% or more of the samples are presented. Bars are ordered by OTU abundance (from most abundant to least abundant) in each sample. Stars indicate sites where carbon uptake microcosms were performed. Eliot and Palmer Glacier are on Mt. Hood; Collier Glacier is on North Sister; the snowfield on Mt. Adams is represented by Mt. Adams; and Gotchen Glacier is on Mt. Adams (sample locations are indicated in Figure 1). SCG; Soil Crenarchaeotic Group; SAGMCG-1; South African Gold Mine Gp 1

Based on BLASTN analyses, the most abundant OTU affiliated with the Soil Crenarchaeotic Group (SCG) was most closely related to sequences recovered from permafrost (Table S7). Sequences affiliated

with the South African Gold Mine Gp 1 (SAGMCG-1) were more abundant on Eliot Glacier which were most closely related to Candidates Nitrosotalea and sequences recovered from the deep hypolimnion of Lake Maggiore (Table S8). Soil Crenarchaeotic Group (SCG) and South African Gold Mine Gp 1 (SAGMCG-1) populations are assumed to contribute to ammonia oxidation in soils. Sequences affiliated with Thermoplasmata were recovered from the sediments from Palmer Glacier and Gotchen Glacier as well as the surface of Gotchen Glacier. The most abundant Thermoplasmata OTUS were most closely related sequences recovered from Lake Taihu and a receding glacier forefield (Table S7).

3.4 | Carbon assimilation

Microcosm assays (in the presence of $NaH^{13}CO_3$) were conducted to examine carbon fixation rates of supraglacial snow (Eliot and Collier glaciers) and periglacial snowfield (Mt. Adams) surfaces. At all sites, little to no bicarbonate was assimilated by assays performed in the dark (Figure 2; Table 2). The highest rates of bicarbonate assimilation ($51\ \mu g\ C\ g^{-1}\ C_{biomass}\ hr^{-1}$) were observed in microcosms performed on Eliot Glacier. Rates of bicarbonate assimilation were lower on Collier Glacier ($6\ \mu g\ C\ g^{-1}\ C_{biomass}\ hr^{-1}$) and on the Mt. Adams snowfield ($15\ \mu g\ C\ g^{-1}\ C_{biomass}\ hr^{-1}$). Photosynthetically active radiation (PAR) fell between ~ 1000 and ~ 1700 $\mu mol\ m^{-2}\ s^{-1}$ throughout the incubation periods (Table S2). At Collier Glacier, PAR values ranged from 1242 to 1696 $\mu mol\ m^{-2}\ s^{-1}$ throughout the incubation period. At Eliot Glacier, values ranging from 1332 to 1542 $\mu mol\ m^{-2}\ s^{-1}$ were observed throughout the incubation period. PAR values were lower during the incubation period on Mt. Adams (ranging from 1003 to 1445 $\mu mol\ m^{-2}\ s^{-1}$). The fluctuation in PAR occurred with changes in minor cloud cover.

Subsets of assays were amended with fixed nitrogen ($NaNO_3$ or NH_4Cl) or phosphorous (as KH_2PO_4). No significant difference was observed in carbon assimilation rates on Mt. Adams in response to amendment with phosphate or nitrate after 60 min or 300 min compared with the control (no amendment, "light") (Figure 3, Table S3). In all microcosms from the Mt. Adams snowfield, the rates of light-dependent carbon assimilation were significantly greater than in the dark treatment (p-value <.05, Table S3). On Eliot Glacier, carbon assimilation rates in the control ("light") were significantly higher than those amended with ammonium (p-value .0003), whereas no difference was observed between the control and phosphate or nitrate (Figure 3, Table S4). Carbon assimilation rates in the phosphate- and nitrate-amended microcosms were significantly higher than the rates in microcosms amended with ammonium (p-values .0000, .0007, respectively; Table S4). Rates were significantly lower in the microcosms covered by the UV block compared with the control as well as those amended with phosphate and nitrate (p-values .0098, .0003, 0.330, respectively; Table S4). Blocking UV radiation also did not result in elevated carbon fixation rates; however, the glass serum vials also blocked all UVB and a portion of UVA radiation as has been observed in other studies (Duarte, Rotter, Malvestiti, & Silva, 2009). Similar to the Mt. Adams snowfield microcosms, rates of carbon assimilation in the dark were significantly lower than all other treatments (p-value <.049; Table S4). At Collier Glacier, there was no significant difference between rates of carbon assimilation in microcosms amended with phosphate, nitrate, or ammonium compared with the control microcosms (Figure 3; Table S5). Similarly, the double amendments of phosphate and nitrate or phosphate and ammonium did not result in significantly elevated carbon assimilation rates compared with the control (Table S5). We also examined bicarbonate uptake in sunlit sediments on Collier Glacier located at the edge of the ice where meltwater left

TABLE 2 Carbon assimilation by snow algae communities[a]

| Site T= | Mt. Adams (snowfield) | | | | Mt. Hood (Eliot) | | North Sister (Collier) | |
| | 60 min $\delta^{15}C$ (‰) | | 300 min $\delta^{13}C$ (‰) | | 135 min $\delta^{13}C$ (‰) | | 390 min $\delta^{13}C$ (‰) | |
	Average	SD	Average	SD	Average	SD	Average	SD
Control	−27.79	0.30	−27.51	0.18	−27.05	1.25	−26.43	0.27
DIC only	−14.42	1.33	29.60	7.91	76.52	7.16	8.78	3.05
PO_4^{3-}	−13.93	1.59	27.18	9.05	86.41	3.60	9.01	3.75
NO_3^-	−15.23	1.61	30.35	0.54	73.35	4.21	23.08	3.32
NH_4^-	−12.80	0.96	27.34	7.10	46.88	6.14	17.81	6.67
UV	−14.34	2.16	41.27	8.11	57.33	7.71	n.d.	
Dark	−27.84	0.11	−26.81	0.52	−26.41	0.60	−23.17	3.99
$NO_3^- + PO_4^{3-}$	n.d.		n.d.		n.d.		5.07	1.26
$NH_4^- PO_4^{3-}$	n.d.		n.d.		n.d.		8.85	9.90
Sediments	n.d.		n.d.		n.d.		52.77	15.50

[a]All carbon isotope values given vs. VPDB.

All carbon isotope values given as absolute values. All samples have ^{13}C-labeled bicarbonate added unless otherwise noted. T, total incubation time; SD, standard deviation ($n = 3$); Control, unlabeled bicarbonate added; DIC only, labeled bicarbonate added; po_4^{3-}, phosphorous added; NO_3^-, nitrate added; NH_4^+, ammonium added; UV, ultraviolet radiation fully blocked; Dark, aluminum foil wrapped; Sediments, supraglacial sediments used for incubation, ^{13}C-labeled bicarbonate added, n.d., not determined.
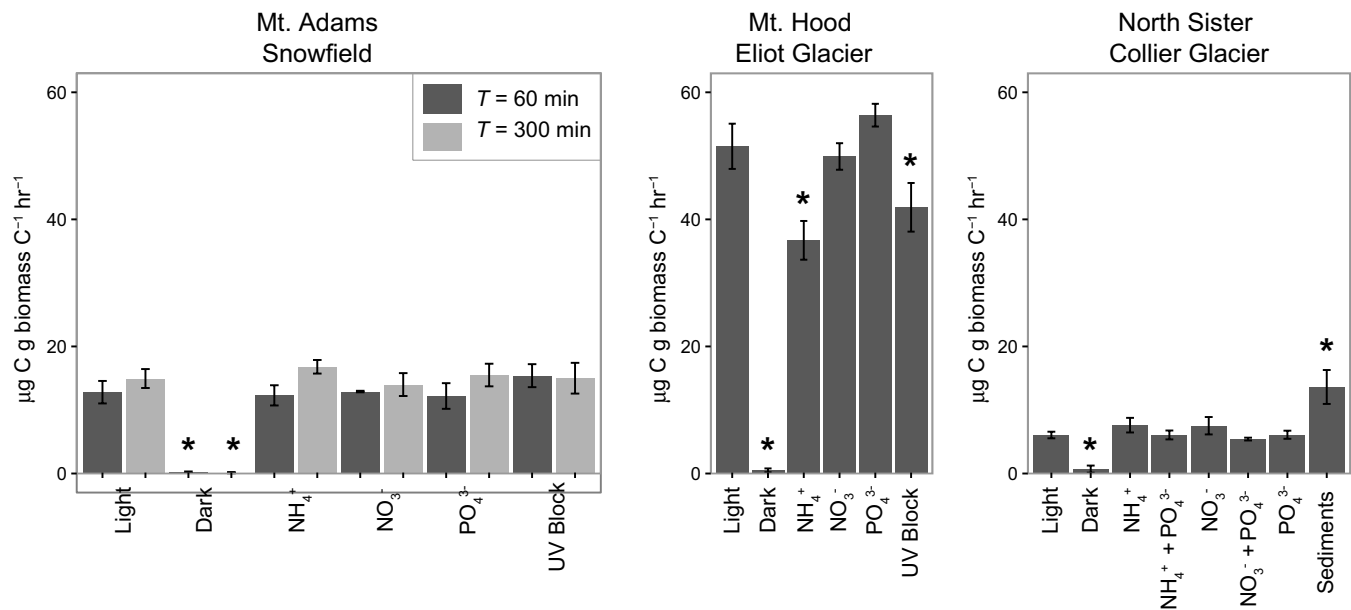
FIGURE 3 Carbon assimilation rates by supraglacial communities. Error bars obtained from triplicate measurements. Asterisks denote carbon assimilation rates that are significantly different than the "light" treatment (*p*-value <.05; Tables S2–S4)

the ice surface. Compared with all other treatments at Collier Glacier, the carbon assimilation rates in the sediment microcosm were significantly higher (*p*-values < .0031; Figure 3; Table S5). As observed in the Mt. Adams snowfield microcosms and the Eliot Glacier microcosms, rates of carbon assimilation in the microcosms incubated in the dark were all significantly less than any other treatment (*p*-values < .0015; Figure 3; Table S5). Based on the recovery of 18S rRNA transcripts affiliated with eukaryotic algae (Figure 2), we assume the majority of inorganic carbon assimilation in the sediments is due to photoautotrophic activity.

4 | DISCUSSION

4.1 | Snow algae communities

4.1.1 | Snow algae

Glacial surfaces are often colored by algal and cyanobacterial blooms both on surface snow and ice and species of algae within the Chlorophyta and bacterial photoautotrophic Cyanobacteria are common in high-alpine snowfields (Morgan-Kiss et al., 2006). Here, we observed 18S rRNA transcripts affiliated with Chlorophyta on the snow and ice surfaces of glaciers in the Pacific Northwest. Chlorophyta are common in high-alpine snowfields and arctic soils (Morgan-Kiss et al., 2006) and have been recovered from glaciers and ice caps. The seven most abundant transcript OTUs (97% identity) we recovered were affiliated with Chlorophyta. Based on BLASTN analyses, five of the seven were most closely related to sequences within the genus *Chlamydomonas* which are typically affiliated with red-colored snow (Hoham & Duval, 2001). Two were affiliated with the genus *Chloromonas*. Species of *Chloromonas*, specifically *Chloromonsa nivalis*, are specially adapted to environmental conditions common on

snowfields and produce secondary carotenoids that result in green-, brownish orange-, or pink-colored snow in both polar and alpine regions (Guiry et al., 2014; Remias et al., 2010). In general, OTUs affiliated with *Chlamydomonas* and *Chloromoans* were more abundant in the supraglacial and periglacial snow samples compared with sediment samples (Table S6). The most abundant, OTU1, was most closely related to *Chlamydomonas* and was abundant in supraglacial snow from Palmer Glacier and Eliot Glacier. OTU2, most closely related to *Chloromonas*, was abundant in supraglacial snow from Palmer Glacier and Gotchen Glacier, whereas OTU4 was most abundant on the snowfield on Mt. Adams. The abundance of transcript OTUs affiliated with photoautotrophic algae is consistent with our observations of significantly higher rates of inorganic carbon assimilation in microcosms exposed to light compared with those incubated in the dark (Figure 3).

4.1.2 | Snow bacteria

The most abundant OTUs we recovered were from 16S rRNA transcripts affiliated with Bacteroidetes and Betaproteobacteria (Figure 2) which are common constituents of snow algae communities (Lutz et al., 2016). The most abundant Bacteroidetes OTUs were affiliated with the genus *Solitalea* and the genus *Ferruginibacter* (Table S7). Species of both *Solitalea* and the genus *Ferruginibacter* are typically heterotrophic. The majority of the Betaproteobacteria 16S rRNA SSU cDNA sequences recovered from the snow and ice samples were affiliated with the order Burkholderiales and the genus *Polaromonas*. *Polaromonas* spp. are commonly observed in samples from glacial surfaces, snow, and sediments (Darcy et al., 2011; Hell et al., 2013; Michaud et al., 2012) and characterized isolates of this genus are typically heterotrophic. The recovery of multiple OTUs most closely related to characterized heterotrophic taxa is consistent

with observations of intense carbon cycling on glacier ice and snow surfaces as has been observed in cryoconite meltholes (Segawa et al., 2014). Our microcosm data are consistent with light-dependent primary production; however, cDNA sequences most closely related to Cyanobacteria (photoautotrophs) were not abundant in any of the samples. These data suggest eukaryotic algae are the dominant primary producers on these snowfields which is consistent with previous observations of algal primary production rates approximately two orders of magnitude higher than bacterial primary production for alpine snowfields (Thomas & Duval, 1995) as well as on the Greenland Ice Sheet (Yallop et al., 2012).

4.1.3 | Snow archaea

We recovered 16S rRNA transcripts affiliated with Archaea from the both ice and snow on the glacier surface and the surrounding sediments. The majority of archaeal OTUs recovered were affiliated with the Thaumarchaeota Soil Crenarchaeota Group (SCG) (Figure 2; Table S8). The SCG is a monophyletic group commonly thought to be ammonia oxidizers. Based on BLASTN analyses, the most abundant archaeal OTU recovered is most closely related to SCG members *Candidatus* Nitrososphaera, *Candidatus* Nitrosoarchaeum, and *Candidatus* Nitrosopelagicus. OTUs affiliated with Thaumarchaeota from Robertson Glacier snow samples were also most closely related to this *Candidate* SCG genus. The recovery of 16S rRNA transcripts affiliated with SCG suggests they are active members of the ice and snow surface ecosystems, consistent with the recovery of closely related transcripts from Robertson Glacier (Hamilton et al., 2013). Sequences affiliated with the Thaumarchaeota were also recovered from cryoconite holes in Antarctica (Cameron, Hodson, & Osborn, 2012); snow in Antarctica (Cameron et al., 2015); and on snow and ice surfaces from glaciers in Iceland (Lutz et al., 2015).

There is evidence that nitrification catalyzed by ammonia-oxidizing bacteria occurs in Arctic snowpack (Amoroso et al., 2010; Hell et al., 2013; Miteva, Sowers, & Brenchley, 2007) and we recovered bacterial transcripts affiliated with Nitrosomonadales, nitrifying bacteria. Functional genes affiliated with both archaeal and bacterial ammonia oxidizers have been recovered from subglacial sediments (Boyd et al., 2011) and observations of nitrification in ex situ microcosm experiments (Skidmore, Foght, & Sharp, 2000; Foght et al., 2004) indicate nitrification occurs in some glacial ecosystems; however, one study of alpine snowpack in the United States did not find evidence of nitrification (Williams, Brooks, Mosier, & Tonnessen, 1996). Our data, along with others, suggest that Thaumarchaeota may be common constituents of supraglacial microbial assemblages and that both AOA and AOB might contribute to N cycling in glacial ecosystems. However, both are present in very low abundance. Ammonia-oxidizing archaea tend to have much higher affinity for reduced nitrogen compared with ammonia-oxidizing bacteria as well as other members of the microbial community (Martens-Habbena, Berube, Urakawa, de la Torre, & Stahl, 2009). Thus, despite the low concentrations of NH_4^+ in glacial ice, snow and meltwater, similar adaptations to low levels of reduced nitrogen might provide ideal niche space for Thaumarchaeota. Isolation of closely related members within the Thaumarchaeota would elucidate much on their role in snow and ice ecosystems.

4.2 | Biogeochemical cycling in supraglacial ecosystems

4.2.1 | Nutrient limitation

Previous studies have suggested that primary productivity by supraglacial communities is limited by nutrients including fixed nitrogen and phosphorous (Edwards et al., 2013; Stibal et al., 2006, 2009; Telling et al., 2011). However, the majority of studies to date have reported rates of carbon fixation in cryoconite meltholes. In our snow algae microcosms, the addition of nitrate, ammonium, or phosphate did not uniformly stimulate carbon fixation (Figure 3). At Collier Glacier, we amended microcosms with a combination of nitrate and phosphate or ammonium and phosphate to examine whether there was evidence for fixed nitrogen and phosphorous colimitation in snow algae communities. Again we did not observe stimulation of carbon fixation in our microcosms. These data suggest the snow algae communities are not limited by fixed nitrogen or phosphorus availability. It is possible that snow algae communities are limited or colimited by other nutrients such as Fe or Mn, that they are mining phosphorous or nitrogen from particles or debris (although nitrogen in rocks is very low), or that they are photoinhibited. Only a few studies have examined photoinhibition of snow algae under in situ conditions and the results are inconclusive and are further complicated by observations that photoinhibiton may vary among snow algae species. In snow algae communities in the Alps of Austria, no photoinhibition was observed at 1800 µmol m^{-2} s^{-1} (Remias, Lütz-Meindl, & Lütz, 2005), whereas other studies suggest subsurface samples that receive less light exhibit elevated levels of photosynthesis suggesting these snow algae communities were not photoinhibited. In our study, we measured photosynthetically active radiation levels between ~1000 and ~1700 µmol m^{-2} s^{-1} throughout the incubations (Table S2) which are consistent with measurements on other glaciers and snowfields where snow algae communities have been observed.

4.2.2 | Carbon cycling

There are relatively few studies that provide ecosystem-scale primary productivity estimates for glacier or snow environments. Here, we observed average carbon assimilation rates ranging between 5.4 and 56.4 µg C g^{-1} C$_{biomass}$ hr^{-1} (Figure 3). These rates are similar to those found for Sierra Nevada snowfields of 7.4–43.9 µg C g^{-1} C$_{biomass}$ hr^{-1} (Thomas & Duval, 1995), converted from µg C cell^{-1} hr^{-1} assuming 6 ng C^{-1} cell^{-1} (Holm-Hanson, 1969). Furthermore, based on a 12-hr day and estimating our sample size of ~0.5 m^2, these rates were similar to those measured for Greenland Ice Sheet cryoconite sites (~4 to 25 µg C g^{-1} C$_{biomass}$ hr^{-1}, assuming a 16-hr day, Hodson et al., 2010) as well as for supraglacial algae (average of ~73 µg C g^{-1} C$_{biomass}$ hr^{-1}, assuming a 16-hr day, Stibal

et al., 2012a,b). Regardless, our data are consistent with photosynthesis driving carbon fluxes on supraglacial and snowfield fluxes (Franzetti et al., 2016).

Natural abundance biomass $\delta^{13}C$ values for the snow algae ranged between −24.1 and −26.9‰, falling within the range of values expected for organisms using the pentose phosphate cycle (i.e., Calvin Cycle) to fix carbon. However, low DIC concentrations precluded determining reliable $\delta^{13}C$ values, so actual fractionation values remain unknown. An approximate $\delta^{13}C$ value of −17.7‰ for the highest DIC concentration site (Gotchen Glacier snow) would suggest a significant fraction of the DIC is sourced from organic material being remineralized by heterotrophs, as DIC sourced from atmospheric CO_2 would have a $\delta^{13}C$ value close to zero (Mook, Bommerson, & Staverman, 1974). This would indicate the algae in the snow near Gotchen Glacier had a fractionation factor ($\delta^{13}C_{DIC}$−$\delta^{13}C_{biomass}$) of only −6.4, suggesting DIC-limiting conditions. Support for the system being DIC-limited is suggested from the low DIC concentrations across all sites (from 13.9 to 84.0 μmol/L), with DOC being anywhere from 2.3 to 7.7 times more abundant. The modest effect of P or fixed N addition to carbon fixation rates provides circumstantial evidence supporting DIC limitation rather than P or fixed N limitation at the sites. Intense carbon cycling has been indicated in cryoconite holes (e.g., Hodson et al., 2010; Telling et al., 2011) and our data suggest supra- and periglacial surfaces are also sites of active carbon cycling. Regardless, while studies suggest supraglacial primary productivity contributes to global carbon cycling, the balance between phototrophic and heterotrophic activity on glacier and snow surfaces remains poorly characterized especially on alpine glaciers and snowfields.

4.2.3 | Nitrogen cycling

Studies of glacial ecosystems and supraglacial snowpack indicate that nitrogen cycling is an important aspect of these ecosystems (Hodson et al., 2008). Anthropogenic input has led to changes in the global nitrogen cycle including an increase in the amount of reactive nitrogen introduced to the atmosphere. While most of this input is thought to affect highly populated regions, it has been predicted that anthropogenic nitrogen has probably influenced watershed nitrogen budgets across the Northern Hemisphere for over a century (Holtgrieve et al., 2011). In fact, anthropogenic changes to the global nitrogen cycle has led to long-range transport of fixed nitrogen compounds that support life such as NO_3^- and NH_4^+ (Dentener et al., 2006; Galloway et al., 2003) to remote locations (Baron, Driscoll, Stoddard, & Richer, 2011; Bergström & Jansson, 2006; Hobbs et al., 2010). Furthermore, this deposition of fixed N to environments that are otherwise pristine or unaltered by human activity may have important impacts on primary productivity (Elser et al., 2009; Higgins, Robinson, Carter, & Pearson, 2010).

Our snow algae biomass $\delta^{15}N$ values were −3.8 to −6.2‰, falling well below values expected for biological nitrogen fixation (~0‰, ±2‰). These negative $\delta^{15}N$ values are consistent with uptake of NH_4^+ and/or NO_3^- sourced from atmospheric deposition (Moore,

1977). Atmospheric N deposition has also been shown to be the strongest control on meltwater nitrogen in glacial systems (Fegel, Baron, Fountain, Johnson, & Hall, 2016). In glacial ecosystems, fixed nitrogen delivered through snowpack will diminish late in the warm season due to snowmelt. In our study, we only observed detectable nitrate concentrations at Palmer and Collier Glaciers and are similar to values found in a recent study of Cascade glaciers where concentrations of nitrate in meltwater were all <10 μM (Fegel et al., 2016). For ice algal communities in Antarctic pack-ice, nitrate was the major nitrogen source for ice algal growth (Kristiansen, Farbrot, Kuosa, Myklestad, & Quillfeldt, 1998); however, uptake of nitrate by algal populations was photoinhibited above an irradiance of >500 μmol m^{-2} s^{-1} (well below the 1000–1700 μmol m^{-2} s^{-1} for this study). In our study, NH_4^+ was below the detection limit of 0.5 μM for all sample sites. In the Fegel et al. study, NH_4^+ was present in all samples, but concentrations were <5 μM. The fact that NH_4^+ and NO_3^- amendment to microcosms did not uniformly stimulate inorganic carbon uptake further suggests C fixation is not fixed N limited (Figure 2). These observations are consistent with delivery of exogenous sources of fixed N to glacial ecosystems as has been observed on seasonal snow in the Rocky Mountains (Williams et al., 1996); glaciers in Svalbard (Hodson et al., 2010) including allochthonous organic carbon rich in organic N (Stibal, Tranter, Benning, & Rehák, 2008); and inferred from nitrogen cycling studies on Robertson Glacier (Boyd et al., 2011).

4.3 | Fe, Mn, and P sequestration in bulk snow algae composition and local bedrock

In volcanic-hosted glaciers such as those in the Cascade Range, mechanisms such as aeolian deposition, rock fall, and fluvial transport deliver ash and comminuted volcanic rock to the snow and ice surface (Figure 4). This transport results in the delivery of elements including Fe, Mn, and P in the form of pulverized volcanic material to snow algae communities. Because glaciers are formed by burial of snowpack, uptake and sequestration of these elements by supraglacial biomass can be buried in glacial ice and subsequently liberated upon melting. To characterize the biomass and associated sediments that would be buried with snow and incorporated into glacial ice, we examined the elemental composition of bulk snow algae community biomass (i.e., all cellular material and associated allochthonous material including volcanic sediments) relative to local rocks. By normalizing element concentrations to aluminum (assumed to be immobile), we identified potential relative enrichments or depletions in particulates associated with the snow algae communities. We assume that elements that are depleted in snow algae samples relative to the local rock have left the system via solubilization and transport as supraglacial or subglacial flow (Figure 4), whereas those that are enriched are sequestered by the snow algae community and are thus potentially more resistant to transport and loss. Comparison of essential nutrients (e.g., Fe, Mn, and P) or biologically neutral (e.g., Mg) elements to Al (an immobile element) indicates that Fe, Mn, and P are all enriched (have ratios that are much higher than that of
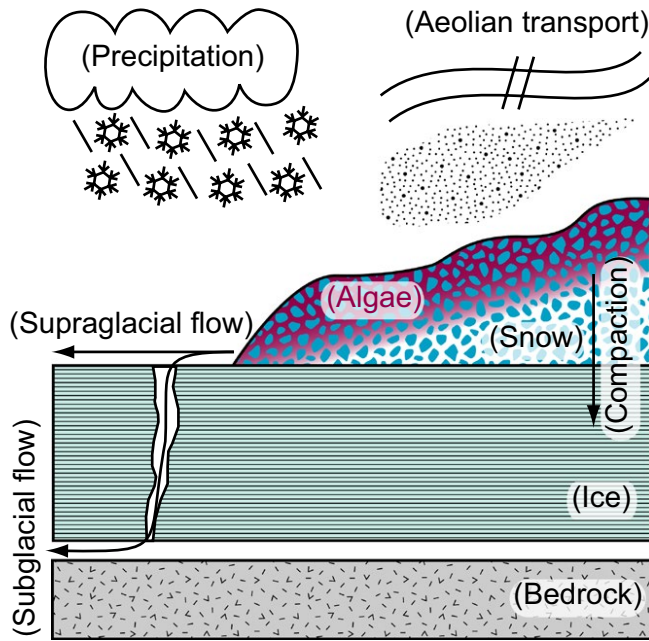
bulk snow algae communities compared with the local lava flows, suggesting the communities are actively breaking down minerals and preferentially sequestering Fe, Mn, and P (either intracellularly or extracellularly), while releasing Mg (as well as Ca, Na, and K) (Figure 5). These observations are consistent with observations of snow algae communities enriched with these elements in Svalbard and the Canadian Arctic (Müller, Bleiß, Martin, Rogaschewski, & Fuhr, 1998; Tazaki et al., 1994) which are presumably delivered by clay aerosols.

Supraglacial biomass is incorporated into the glacier as ice during times of glacial growth. We expect the burial of snow algae communities to result in glacial ice that is enriched in Fe, Mn, and P (as well as organic material including C and N). This enrichment likely varies between glacial ecosystems due to differences in aeolian deposition, rock fall, and fluvial transport. Regardless, these nutrients will eventually be released upon glacial melt, providing nutrients to subglacial and down-drainage communities. Snow algae communities play an important role in supraglacial and periglacial snow food webs and supply nutrients that will be delivered throughout the glacial ecosystem. Variation in delivery of nutrients to the surface affects the rates of primary productivity which feeds into local heterotrophic pathways and aids in supporting downstream (and subglacial ecosystems). However, the delivery of nutrients from buried snow biomass is not usually considered in glacial ecosystem food webs. Our data suggest buried snow algae biomass could be an important source of C, N, Fe, Mn, and P upon melt and glacial retreat.
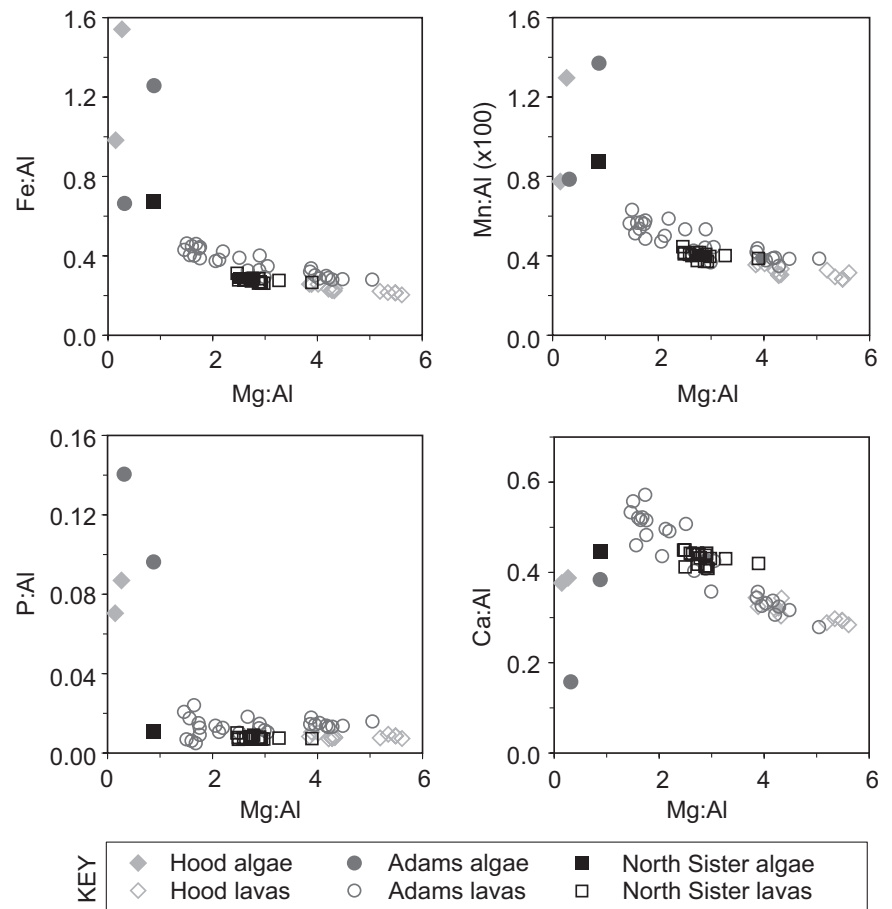

FIGURE 4 Conceptual model of precipitation, aeolian deposition, and fluvial transport delivering material to snow algae communities

local lava flows) when compared to the ratios measured by previous work on lava flows at Mt. Hood (Cribb & Barton, 1997), Mt. Adams (Jicha et al., 2009), and North Sister (Schmidt & Grunder, 2011). In contrast, Mg and Ca exhibit depletion relative to aluminum in the

FIGURE 5 Ratios of essential nutrients and biologically neutral elements to aluminum in snow algae biomass and local lava flows. All algae samples fall below the 1:1 Mg concentration:Al concentration ratio, and all rock values fall above this ratio. Lava geochemistry values collected from Cribb and Barton (1997), Jicha et al. (2009), and Schmidt and Grunder (2011)

5 | CONCLUSIONS

Here, we present carbon fixation rates and the community structure of the active fraction of snow algae communities on supraglacial and periglacial snow of the Pacific Northwest that are hosted in volcanic terrains. Our data highlight a role for local bedrock in delivering nutrients to ice and snow communities as well as the sequestration of biologically important elements by supraglacial biomass. In contrast to other studies, our data do not support fixed nitrogen or phosphorous limitation of supraglacial primary productivity. Instead, our data suggest DIC may be limiting although we cannot rule out photoinhibiton or colimitation by a combination of essential elements. These studies underscore the need for similar studies in other bedrock geologies to better constrain biogeochemical cycling on glaciers and snowfields and the subsequent delivery of nutrients to downstream ecosystems including the subglacial sediments.

REFERENCES

Altschul, S. F., Madden, T. L., Schäffer, A. A., Zhang, J., Zhang, Z., Miller, W., & Lipman, D. J. (1997). Gapped BLAST and PSI-BLAST: A new generation of protein database search programs. *Nucleic Acids Research, 25*, 3389–3402.

Amoroso, A., Domine, F., Esposito, G., Morin, S., Savarino, J., Nardino, M., Montagnoli, M., … Beine, H. J. (2010). Microorganisms in dry polar snow are involved in the exchanges of reactive nitrogen species with the atmosphere. *Environmental Science & Technology, 44*, 714–719. doi:10.1021/es9027309

Anesio, A. M., Hodson, A. J., Fritz, A., Penner, R., & Sattler, B. (2008). High microbial activity on glaciers: Importance to the global carbon cycle. *Global Change Biology, 15*, 955–960. doi:10.1111/j.1365-2486.2008.01758.x

Apprill, A., McNally, S., Parsons, R., & Weber, L. (2015). Minor revision to V4 region of SSU rRNA 806R gene primer greatly increases detection of SAR11 bacterioplankton. *Aquatic Microbial Ecology, 75*, 129–137. doi:10.3354/ame01753

Baron, J. S., Driscoll, C. T., Stoddard, J. L., & Richer, E. E. (2011). Empirical critical loads of atmospheric nitrogen deposition for nutrient enrichment and acidification of sensitive US lakes. *BioScience, 61*, 602–612. doi:10.1525/bio.2011.61.8.6

Bergström, A.-K., & Jansson, M. (2006). Atmospheric nitrogen deposition has caused nitrogen enrichment and eutrophication of lakes in the northern hemisphere. *Global Change Biology, 12*, 635–643. doi:10.1111/j.1365-2486.2006.01129.x

Boetius, A., Anesio, A. M., Deming, J. W., Mikucki, J. A., & Rapp, J. Z. (2015). Microbial ecology of the cryosphere: Sea ice and glacial habitats. *Nature Reviews Microbiology, 13*, 677–690. doi:10.1038/nrmicro3522

Boyd, E. S., Hamilton, T. L., Havig, J., Skidmore, M. L., & Shock, E. S. (2014). Chemolithotrophic primary production in a subglacial ecosystem. *Applied and Environmental Microbiology, 80*, 6146–6153. doi:10.1128/AEM.01956-14

Boyd, E. S., Lange, R. K., Mitchell, A. C., Havig, J. R., Hamilton, T. L., Lafrenière, M. J., … Skidmore, M. (2011). Diversity, abundance, and potential activity of nitrifying and nitrate-reducing microbial assemblages in a subglacial ecosystem. *Applied Environmental Microbiology, 77*, 4778–4787. doi:10.1128/AEM.00376-11

Branda, E., Turchetti, B., Diolaiuti, G., Pecci, M., Smiraglia, C., & Buzzini, P. (2010). Yeast and yeast-like diversity in the southernmost glacier of Europe (Calderone Glacier, Apennines, Italy). *FEMS Microbiology Ecology, 72*, 354–369. doi:10.1111/j.1574-6941.2010.00864.x

Brown, S. O., Ungerer, M. C., & Jumpponen, A. (2016). A community of clones: Snow algae are diverse communities of spatially structured clones. *International Journal of Plant Sciences, 177*, 5. doi: 10.1086/686019

Cameron, K. A., Hagedorn, B., Dieser, B. C., Christner, B. C., Choquette, K., Sletten, R., … Junge, K. (2015). Diversity and potential sources of microbiota associated with snow on western portions of the Greenland Ice Sheet. *Environmental Microbiology, 17*, 694–609. doi:10.1111/1462-2920.12446

Cameron, K. A., Hodson, A. J., & Osborn, A. M. (2012). Structure and diversity of bacterial, eukaryotic and archaeal communities in glacial cryoconite holes from the Arctic and the Antarctic. *FEMS Microbiology Ecology, 82*, 254–267. doi:10.1111/j.1574-6941.2011.01277.x

Caporaso, J. G., Lauber, C. L., Walters, W. A., Berg-Lyons, D., Huntley, J., Fierer, N., … Knight, R. (2012). Ultra-high-throughput microbial community analysis on the Illumina HiSeq and MiSeq platforms. *The ISME Journal, 6*, 1621–1624. doi:10.1038/ismej.2012.8

Cook, J. M., Hodson, A. J., Anesio, A. M., Hanna, E., Yallop, M., Stibal, M., … Huybrechts, P. (2012). An improved estimate of microbially mediated carbon fluxes from the Greenland ice sheet. *Journal Glaciology, 58*, 1098–1108. doi:10.3189/2012JoG12J001

Cribb, J. W., & Barton, M. (1997). Significance of crustal and source region processes on the evolution of compositionally similar calc-alkaline lavas, Mt. Hood, Oregon. *Journal of Volcanology and Geothermal Research, 76*, 229–249. doi:10.1016/S0377-0273(96)00077-7

Darcy, J. L., Lynch, R. C., King, A. J., Robeson, M. S., & Schmidt, S. K. (2011). Global distribution of Polaromonas phylotypes—evidence for a highly successful dispersal capacity. *PLoS ONE, 6*, e23742. doi:10.1371/journal.pone.0023742

Dentener, F, Drevet, J, Lamarque, JF, Bey, I, Eickhout, B, Fiore, AM, & Szopa, S (2006) Nitrogen and sulfur deposition on regional and global scales: A multimodel evaluation. *Global Biogeochemical Cycles 20*:GB4003. doi: 10.1029/2005GB002672

Duarte, I., Rotter, A., Malvestiti, A., & Silva, M. (2009). The role of glass as a barrier against the transmission of ultraviolet radiation: An experimental study. *Photodermatology, Photoimmunology & Photomedicine, 25*, 181–184. doi:10.1111/j.1600-0781.2009.00434.x

Edgar, R. C., Haas, B. J., Clemente, J. C., Quince, C., & Knight, R. (2011). UCHIME improves sensitivity and speed of chimera detection. *Bioinformatics, 27*, 2194–2200. doi:10.1093/bioinformatics/btr381

Edwards, A., Pachebat, J. A., Swain, M., Hegarty, M., Hodson, A. J., Irvine-Flynn, T. D. L., … Sattler, B. (2013). A metagenomic snapshot of taxonomic and functional diversity in an alpine glacier cryoconite ecosystem. *Environmental Research Letters, 8*, 035003. doi:(10.1088/1748-9326/8/3/035003)

Elser, J. J., Anderson, T., Baron, J. S., Bergström, A.-K., Jansson, M., Kyle, M., … Hessen, D. O. (2009). Shifts in lake N: P stoichiometry and nutrient limitation driven by atmospheric nitrogen deposition. *Science, 326*, 835–837. doi:10.1126/science.1176199 pmid:19892979

Fegel, T. S., Baron, J. S., Fountain, A. G., Johnson, G. F., & Hall, E. K. (2016). The differing biogeochemical and microbial signatures of glaciers and rock glaciers. *Journal of Geophysical Research - Biogesciences, 121*, 919–923. doi: 10.1002/2015JG003236

Foght, J., Aislabie, J., Turner, S., Brown, C. E., Ryburn, J., Saul, D. J., & Lawson, W. (2004). Culturable bacteria in subglacial sediments and ice from two southern hemisphere glaciers. *Microbial Ecology*, *47*, 329–340. doi: 10.1007/s00248-003-1036-5

Franzetti, A, Tagliaferri, I, Gandolfi, I, Bestetti, G, Minoa, U, Mayer, C, … Ambrosin, R (2016). Light-dependent microbial metabolisms drive carbon fluxes on glacier surfaces. *The ISME Journal*. doi: 10.1038/ismej.2016.72. [Epub ahead of print].

Fujii, M., Takano, Y., Kojima, H., Hoshino, T., Tanaka, R., & Fukui, M. (2010). Microbial community structure, pigment composition and nitrogen source of red snow in Antarctica. *Microbial Ecology*, *59*, 466–475. doi:10.1007/s00248-009-9594-9

Galloway, J. N., Aber, J. D., Erisman, J. W., Seitzinger, S. P., Howarth, R. W., Cowling, E. B., & Cosby, B. J. (2003). The nitrogen cascade. *BioScience*, *53*, 341–356. doi:10.1641/0006-3568(2003) 053[0341:TNC]2.0.CO;2

Guiry, M. D., Guiry, G. M., Morrison, L., Rindi, F., Valenzuela, S., Miranda, A. C., … Garbary, D. J. (2014). AlgaeBase: An on-line resource for Algae. *Cryptogamie, Algologie*, *35*, 105–115. doi:10.7872/crya.v35.iss2.2014.105

Hamilton, T. L., Peters, J. W., Skidmore, M. L., & Boyd, E. S. (2013). Molecular evidence for an active endogenous microbiome beneath glacial ice. *The ISME Journal*, *7*, 1402–1412. doi:10.1038/ismej.2013.31

Havig, J., Raymond, J., Meyer-Dombard, D. R., Zolotova, N., & Shock, E. L. (2011). Merging isotopes and community genomics in a siliceous sinter-depositing hot spring. *Journal Geophysical Research*, *116*, G01005. doi:(10.1029/2010JG001415)

Hell, K., Edwards, A., Zarsky, J., Podmirseg, S. M., Girdwood, S., Pachebat, J. A., … Sattler, B. (2013). The dynamic bacterial communities of a melting High Arctic glacier snowpack. *The ISME Journal*, *7*, 1814–1826. doi:10.1038/ismej.2013.51

Higgins, M. B., Robinson, R. S., Carter, S. J., & Pearson, A. (2010). Evidence from chlorin nitrogen isotopes for alternating nutrient regimes in the Eastern Mediterranean Sea. *Earth and Planetary Science Letters*, *290*, 102–107. doi:10.1016/j.epsl.2009.12.009

Hildreth, W., & Lanphere, M. A. (1994). Potassium-argon geochronology of a basaltic-dacite arc system: The Mount Adams volcanic field, Cascade Range of southern Washington. *Geological Society of America Bulletin*, *106*, 1413–1429.

Hisakawa, N, Quistad, SD, Hester, ER, Martynova, D, Maughan, H, Sala, E, … Rohwer, F (2015). Metagenomic and satellite analyses of red snow in the Russian Arctic. *PeerJ*, *3*, e1491 doi: https://doi.org/10.7717/peerj.1491.

Hobbs, W. O., Telford, R. J., Birks, J. B., Saros, J. E., Hazewinkel, R. R. O., Perren, B. B., … Wolde, A. E. (2010). Quantifying recent ecological changes in remote lakes of North America and Greenland using sediment diatom assemblages. *PLoS ONE*, *5*, e10026. doi:(10.1371/journal.pone.0010026 pmid:20368811)

Hodson, A., Anesio, A. M., Tranter, M., Fountain, A., Osborn, M., Priscu, J., … Sattler, B. (2008). Glacial ecosystems. *Ecological Monographs*, *78*, 41–67. doi:(10.1890/07-0187.1)

Hodson, A., Bøggild, C., Hanna, E., Huybrechts, P., Langford, H., Cameron, K., & Houldsworth, A. (2010). The cryoconite ecosystem on the Greenland ice sheet. *Annals of Glaciology*, *51*, 123–129. doi:10.3189/172756411795931985

Hoham, R. W., & Duval, B. (2001). Microbial ecology of snow and freshwater ice with emphasis on snow algae. In H. G. Jones, J. W. Pomeroy, D. A. Walker, & R. W. Hoham (Eds.), *Snow Ecology: An Interdisciplinary Examination of Snow-covered Ecosystems* (pp. 168–228). Cambridge, UK: Cambridge University Press.

Holm-Hanson, O. (1969). Algae: amounts of DNA and organic carbon in single cells. *Science*, *163*, 87–88. doi: 10.1126/science.163.3862.87

Holtgrieve, G. W., Schindler, D. E., Hobbs, W. O., Leavitt, P. R., Ward, E. J., Bunting, L., … Wolfe, A. P. (2011). A coherent signature of anthropogenic nitrogen deposition to remote watersheds of the northern hemisphere. *Science*, *334*, 1545–1548. doi:10.1126/science.1212267

Jackson, K. M., & Fountain, A. G. (2007). Spatial and morphological change on Eliot Glacier, Mount Hood, Oregon, USA. *Annals of Glaciology*, *46*, 222–226. doi:10.3189/172756407782871152

Jicha, B. R., Johnson, C. M., Hildreth, W., Beard, B. L., Hart, G. L., Shirey, S. B., & Singer, B. S. (2009). Discriminating assimilants and decoupling deep-vs. shallow-level crystal records at Mount Adams using 238 U–230 Th disequilibria and Os isotopes. *Earth and Planetary Science Letters*, *277*, 38–49. doi:(10.1016/j.epsl.2008.09.035)

Klassen, J. L., Foght, JM (2011). Characterization of Hymenobacter isolates from Victoria Upper Glacier, Antarctica reveals five new species and substantial non-vertical evolution within this genus. *Extremophiles*, *15*, 45–57. doi: 10. 1007/s00792-010-0336-1

Kozich, J. J., Westcott, S. L., Baxter, N. T., Highlander, S. K., & Schloss, P. D. (2013). Development of a dual-index sequencing strategy and curation pipeline for analyzing amplicon sequence data on the MiSeq Illumina sequencing platform. *Applied and Environmental Microbiology*, *79*, 5112–5120. doi:10.1128/AEM.01043-13

Kristiansen, S., Farbrot, T., Kuosa, H., Myklestad, S., & Quillfeldt, C. H. (1998). Nitrogen uptake in the infiltration community, an ice algal community in Antarctic pack-ice. *Polar Biology*, *19*, 307–315.

Lutz, S., Anesio, A. M., Edwards, A., & Benning, L. G. (2015). Microbial diversity on Icelandic glaciers and ice caps. *Frontiers in Microbiology*, *6*, 307. doi:(10.3389/fmicb.2015.00307)

Lutz, S., Anesio, A. M., Raiswell, R., Edwards, A., Newton, R. J., Gill, F., & Benning, L. G. (2016). The biogeography of red snow microbiomes and their role in melting arctic glaciers. *Nature Communications*, *7*, 11968. doi:(10.1038/ncomms11968)

Martens-Habbena, W., Berube, P. M., Urakawa, H., de la Torre, J. R., & Stahl, D. A. (2009). Ammonia oxidation kinetics determine niche separation of nitrifying Archaea and Bacteria. *Nature*, *461*, 976–979. doi:10.1038/nature08465

McMurdie, P. J., & Holmes, S. (2013). phyloseq: An R package for reproducible interactive analysis and graphics of microbiome census data. *PLoS ONE*, *8*, e61217. doi:(10.1371/journal.pone.0061217)

Mercer, C. N., & Johnston, A. D. (2008). Experimental studies of the P-T–H2O near-liquidus phase relations of basaltic andesite from North Sister Volcano, High Oregon Cascades: Constraints on lower-crustal mineral assemblages. *Contributions to Mineralogy and Petrology*, *155*, 571–592. doi:10.1007/s00410-007-0259-8

Michaud, L., Caruso, C., Mangano, S., Interdonato, F., Bruni, V., & Lo Giudice, A. (2012). Predominance of Flavobacterium, Pseudomonas, and Polaromonas within the prokaryotic community of freshwater shallow lakes in the northern Victoria Land, East Antarctica. *FEMS Microbiology Ecology*, *82*, 391–404. doi:10.1111/j.1574-6941.2012.01394.x

Miteva, V., Sowers, T., & Brenchley, J. (2007). Production of N_2O by ammonia oxidizing bacteria at subfreezing temperatures as a model for assessing the N_2O anomalies in the Vostok ice core. *Geomicrobiology Journal*, *24*, 451–459. doi:10.1080/01490450701437693

Mook, W. G., Bommerson, J. C., & Staverman, W. H. (1974). Carbon isotope fractionation between dissolved bicarbonate and gaseous carbon dioxide. *Earth and Planetary Science Letters*, *22*, 169–176.

Moore, H. (1977). The isotopic composition of ammonia, nitrogen dioxide and nitrate in the atmosphere. *Atmospheric Environment*, *11*, 1239–1243.

Morgan-Kiss, R. M., Priscu, J. C., Pocock, T., Gudynaite-Savitch, L., & Huner, N. P. A. (2006). Adaptation and Acclimation of Photosynthetic Microorganisms of Permanently Cold Environments. *Microbiology and Molecular Biology Reviews*, *70*, 222–252. doi:10.1128/MMBR.70.1.222-252.2006

Müller, T., Bleiß, W., Martin, C. D., Rogaschewski, M. S., & Fuhr, G. (1998). Snow algae from northwest Svalbard: Their identification, distribution, pigment and nutrient content. *Polar Biology*, *20*, 14–32.

Remias, D., Karsten, U., Lütz, C., & Leya, T. (2010). Physiological and morphological processes in the Alpine snow alga *Chloromonas*

nivalis (Chlorophyceae) during cyst formation. *Protoplasma*, 243, 73–86. doi:10.1007/s00709-010-0123-y

Remias, D., Lütz-Meindl, U., & Lütz, C. (2005). Photosynthesis, pigments and ultrastructure of the alpine snow alga *Chlamydomonas nivalis*. *European Journal of Phycology*, 40, 259–268. doi:10.1080/09670260500202148

Schloss, P. D., Westcott, S. L., Ryabin, T., Hall, J. R., Hartmann, M., Hollister, E. B., … Weber, C. F. (2009). Introducing mothur: Open-source, platform-independent, community-supported software for describing and comparing microbial communities. *Applied and Environmental Microbiology*, 75, 7537–7541. doi:10.1128/AEM.01541-09

Schmidt, M. E., & Grunder, A. L. (2011). Deep mafic roots to arc volcanoes: Mafic recharge and differentiation of basaltic andesite at North Sister Volcano, Oregon Cascades. *Journal of Petrology*, 52, 603–641. doi:10.1093/petrology/egq094

Segawa, T., Ishii, S., Ohte, N., Akiyoshi, A., Yamada, A., Maruyama, F., … Takeuchi, N. (2014). The nitrogen cycle in cryoconites: Naturally occurring nitrification-denitrification granules on a glacier. *Environmental Microbiology*, 16, 3250–3262. doi:10.1111/1462-2920.12543

Sitts, D. J., Fountain, A. G., & Hoffman, M. J. (2010). Twentieth Century Glacier Change on Mount Adams, Washington, USA. *Northwest Science (Northwest Scientific Association)*, 84, 378–385. doi:10.3955/046.084.0407

Skidmore, M. L., Foght, J. M., & Sharp, M. J. (2000). Microbial life beneath a high arctic glacier. *Applied and Environmental Microbiology*, 66, 3214–3220. doi:10.1128/AEM.66.8.3214-3220.2000

Stibal, M., Anesio, A. M., Blues, C. J. D., & Tranter, M. (2009). Phosphatase activity and organic phosphorus turnover on a high Arctic glacier. *Biogeosciences*, 6, 913–922. doi:10.5194/bg-6-913-2009

Stibal, M., Šabacká, M., & Kaštovská, K. (2006). Microbial communities on glacier surfaces in Svalbard: impact of physical and chemical properties on abundance and structure of cyanobacteria and algae. *Microbial Ecology*, 52, 644–654. doi:10.1007/s00248-006-9083-3

Stibal, M., Šabacká, M., & Žársky, J. (2012a). Biological processes on glacier and ice sheet surfaces. *Nature Geosciences*, 5, 771–774. doi:10.1038/ngeo1611

Stibal, M., Telling, J., Cook, J., Mak, K. M., Hodson, A., & Anesio, A. M. (2012b). Environmental controls on microbial abundance and activity on the Greenland ice sheet: A multivariate analysis approach. *Microbial Ecology*, 63, 74–84. doi:10.1007/s00248-011-9935-3

Stibal, M., Tranter, M., Benning, L. G., & Rehák, J. R. (2008). Microbial primary production on an Arctic glacier is insignificant in comparison with allochthonous organic carbon input. *Environmental Microbiology*, 10, 2172–2178. doi:10.1111/j.1462-2920.2008.01620.x

Takeuchi, N., Dial, R., Kohshima, S., Segawa, T., & Uetake, J. (2006). Spatial distribution and abundance of red snow algae on the Harding Icefield, Alaska derived from a satellite image. *Geophysical Research Letters*, 33, L21502. doi:(10.1029/2006GL027819)

Tazaki, K., Fyfe, W. S., Iizumi, S., Sampei, Y., Watanabe, H., Goto, M., … Noda, S. (1994). Clay aerosols and arctic ice algae. *Clays and Clay Minerals*, 42, 402–408.

Telling, J., Anesio, A. M., Tranter, M., Irvine-Fynn, T., Hodson, A., Butler, C., & Wadham, J. (2011). Nitrogen fixation on Arctic glaciers. *Svalbard. Journal of Geophysical Research*, 116, G03039. doi:(10.1029/2010JG001632)

Thomas, W. H., & Duval, B. (1995). Sierra-Nevada, California, USA, snow algae—snow albedo changes, algal bacterial interrelationships, and ultraviolet-radiation effects. *Arctic Antarctic and Alpine Research*, 27, 389–399.

Weekers, P. H. H., Gast, R. J., Fuerst, P. A., & Byers, T. J. (1994). Sequence variations in small-subunit ribosomal RNAs of Hartmannella vermiformis and their phylogenetic implications. *Molecular Biology and Evolution*, 11, 684–690.

Williams, M. W., Brooks, P. D., Mosier, A., & Tonnessen, K. A. (1996). Mineral nitrogen transformations in and under seasonal snow in a high-elevation catchment in the Rocky Mountains, United States. *Water Resources Research*, 32, 3161–3171. doi:10.1029/96WR02240

Wise, W. S. (1969). Geology and petrology of the Mt. Hood area: A study of high Cascade volcanism. *Geological Society of America Bulletin*, 80, 969–1006.

Yallop, M. L., Anesio, A. M., Perkins, R. G., Cook, J., Telling, J., Fagan, D., … Bellas, C. (2012). Photophysiology and albedo-changing potential of the ice algal community on the surface of the Greenland ice sheet. *The ISME Journal*, 6, 2302–2313. doi:10.1038/ismej.2012.107

Zhang, S., Yang, G., Wang, Y., & Hou, S (2009). Abundance and community of snow bacteria from three glaciers in the Tibetan Plateau. *Journal of Environmental Sciences*, 22, 1418–1424. doi: 10.1016/S1001-0742(09)60269-2

SUPPORTING INFORMATION

Additional Supporting Information may be found online in the supporting information tab for this article.